Trap loss in a metastable helium-rubidium magneto-optical trap

L. J. Byron,[*] R. G. Dall, and A. G. Truscott

ARC Centre of Excellence for Quantum-Atom Optics and Research School of Physical Sciences and Engineering,
Australian National University, Canberra ACT-0200, Australia

We present results of the study of a simultaneously confined metastable helium (He*) and rubidium magneto-optical trap (MOT). By monitoring the trap decay of the ^{87}Rb MOT with and without a He* MOT present, we find the light-assisted, two-body loss rate to be $\beta_{\text{Rb-He}^*} = (6 \pm 2) \times 10^{-10}$ cm^3/s. Moreover, we find that it is possible to create a large, robust ^{87}Rb-He* MOT, opening the possibility of creating a ^{87}Rb-He* Bose-Einstein condensate. This would be the first dual-species condensate incorporating an alkali metal ground-state atom and an excited-state noble gas atom.

I. INTRODUCTION

Multispecies cold-atom traps are an exciting and relatively new area of research. They provide an excellent environment to study cold collisions between two different species, including both inelastic [1] and elastic processes [2]. They can be used to create exotic heteronuclear molecules [3] and are usually the first step in the creation of dual-species Bose-Einstein condensates (BECs) [4].

We present here a realization of a dual-species system consisting of metastable helium (He*) and another species, ^{87}Rb, in a magneto-optical trap (MOT). Nearly all previous experiments have involved various alkali-metal–alkali-metal combinations such as Na-K, Li-Cs, Cs-K [5], and Cr-^{87}Rb [6]. There has been just one alkali-metal-metastable experiment to date, and this experiment involved metastable argon and ^{85}rubidium [7]. Unlike the ^{85}Rb-Ar* MOT experiment, both ^{87}Rb and He* are individually condensable, allowing for the very real possibility of creating the first dual-species, alkali-metal-metastable BEC.

A ^{87}Rb-He* system combines two species with very different atomic characteristics, and their robust coexistence is not a foregone conclusion. He* has a very simple atomic structure, a large magnetic moment, is very light, and most importantly has a large internal energy ~20 eV. ^{87}Rb, however, has a much more complicated atomic structure, a lower magnetic moment, is much heavier than He*, and is in its ground state. This combination opens a fascinating avenue for future experiments. First, as there is no hyperfine structure in He*, it is possible to study in detail hyperfine-state changing collisions in just one of the collision partners. Second, in a ^{87}Rb-He* MOT, it is possible to cool ^{87}Rb to 10 μK using polarization gradient cooling techniques [8]. If elastic/inelastic collision rates prove favorable, sympathetic cooling should be possible, allowing He* to thermalize to a temperature of ~10 μK. This is only a factor of 2 above the highest He* condensation temperature previously reported [9]. Thus, it may be possible to create a large number He* condensate. Finally, if the loss rates are suitably low, a ^{87}Rb-He* condensate may be possible. Two species condensates offer the opportunity to study more complex structures and fascinating

new phenomena that do not exist in single-species condensates. However, to date, only alkali-metal–alkali-metal condensates have been experimentally realized. Realization of a ^{87}Rb-He* condensate would also pave the way for an attempt to create exotic ultracold ^{87}Rb-He* molecules as well as to investigate interspecies Feshbach resonances.

All of these experiments rely on a large and robust ^{87}Rb-He* MOT. A large MOT is only possible if the inelastic loss rate is low. Thus, measuring the light-assisted, two-body loss rate $\beta_{\text{Rb-He}^*}$, as is reported here, is important. There are reasons to believe that this loss rate could be large. He* with its large internal energy of 19.8 eV is capable of ionizing most atoms and molecules that it collides with in a process known as Penning ionization

$$\text{He}^* + A \rightarrow \text{He} + A^+ + e^-. \tag{1}$$
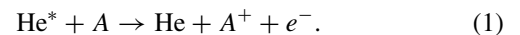
^{87}Rb atoms have an ionization energy of ~4 eV and thus are readily Penning ionized by a He* atom. Such a collision results in the loss of both atoms from the trap and could severely limit the lifetime of a ^{87}Rb-He* MOT. The lifetime of a He* MOT is usually dominated by this process as is seen by the very high two-body loss rate. The He* light-assisted, two-body loss has previously been measured as $1.9 \pm 0.8 \times 10^{-9}$ cm^3/s [10]. This is approximately three orders of magnitude greater than the light-assisted, two-body loss rate for ^{87}Rb of $3.7 \pm 1.7 \times 10^{-12}$ cm^3/s [11].

II. EXPERIMENTAL APPARATUS

Separate laser systems and optics are used for each atomic species. He* is cooled and trapped using the 1083 nm $2^3S_1 \rightarrow 2^3P_2$ transition, whereas ^{87}Rb is cooled and trapped using the 780 nm $5P_{1/2}F = 2 \rightarrow 5P_{3/2}F = 3$ transition and "repumped" using the 780 nm $5P_{1/2}F = 1 \rightarrow 5P_{3/2}F = 2$ transition. An energy-level diagram for both atoms is shown in Fig. 1.

The ^{87}Rb-He* MOT is produced in a stainless-steel, commercially available, 8″ spherical octagon Kimball physics chamber attached to an extensive vacuum system. The experimental setup has been designed such that the background pressure in this chamber is at a minimum ~10^{-10} torr, as future BEC experiments are planned that require a very low background pressure.
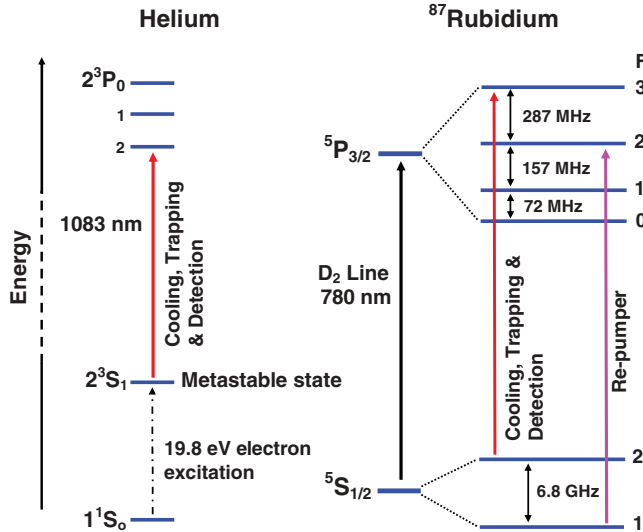
---

[*]Lesa.Byron@anu.edu.au

FIG. 1. (Color online) Simplified energy-level diagrams for He* and ^{87}Rb showing the laser transitions utilized.

FIG. 2. (Color online) Simplified MOT diagram with the beam layout. The patterned (blue) beams represent the ^{87}Rb laser beams, whereas the solid (red) beams represent He* laser beams.

The He* MOT is loaded from a typical beamline system. The He* is produced in a liquid-nitrogen-cooled dc discharge source [12], collimated with a two-dimensional optical molasses and slowed with a Zeeman slower to ~70 m/s, at which point the atoms can be loaded into a MOT [13]. Metastable dc discharge sources are extremely inefficient, ~0.01% [14]. They produce a high background of ground-state He atoms, ions, electrons, and so on, that copropagate with the He* beam. This background causes a large single-body loss of atoms from the ^{87}Rb MOT. To isolate the main MOT chamber from this background, an *in vacuo* valve is placed at the end of the Zeeman slower. With the *in vacuo* valve open and the He* source in operation, the pressure in the chamber is ~1×10^{-9} torr (however, the local pressure at the chamber center is probably much higher due to line of sight to the source). With the *in vacuo* valve closed, the pressure drops to ~10^{-10} torr.

^{87}Rb is produced from a commercial Alvatec alkali-metal vapor dispenser placed in a smaller source chamber separated from the main chamber by a differential pumping stage. We obtain peak flux when the dispensers are operated continuously at a pressure of ~10^{-9} torr. To extract the ^{87}Rb into the main chamber, a low-velocity intense source (LVIS), similar in design to [15], is used to push the atoms through the differential pumping stage. The LVIS consists of three nonidentical, retro-reflected ($\sigma^+ - \sigma^-$ polarization) orthogonal beams with detuning $\delta = -3\Gamma$. Two of these beams are ~35 mm in diameter with an intensity of ~10 mW/cm^2 and are retro-reflected with optics outside the chamber. The third is ~10 mm in diameter with an intensity of ~12 mW/cm^2 and is retro-reflected with a mirror and waveplate placed inside the source chamber in front of the differential pumping tube. These internal optics have a ~1-mm hole in their center that casts a shadow on the axis of the reflected beam. Atoms in this shadow are "pushed" through the hole and the differential pumping stage into the main chamber. A pair of anti-Helmholtz coils generates the quadrupole magnetic field required for the LVIS, with a gradient of 10 G/cm. Approximately 500 μW
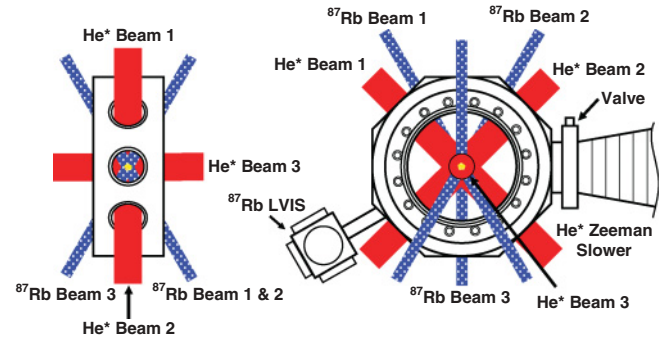
of repumping light is overlapped with one of the large beams. The LVIS loads a ^{87}Rb MOT with ~1×10^8 atoms/s.

As the laser wavelengths needed for cooling and trapping are vastly different, a separate set of optics is needed for each MOT. This has the advantage of permitting independent control of the placement of each MOT, allowing optimal overlap of the clouds to be achieved. The He* MOT consists of three orthogonal retro-reflected beams with a diameter of ~35 mm, an intensity of 30 mW/cm^2, and a detuning of $\delta = -20\Gamma$.

The ^{87}Rb MOT also consists of three retro-reflected beams; however, these could not be placed in the traditional orthogonal setup due to access constraints; instead the beams are in a 60° configuration (see Fig. 2). While not an optimal configuration, a sufficient number of ^{87}Rb atoms can be trapped. The ^{87}Rb MOT beams have a diameter of ~10 mm, an intensity of 7 mW/cm^2, and a detuning of $\delta = -2\Gamma$.

The magnetic field is produced by a pair of coils in an anti-Helmholtz configuration, and a gradient of ~10 G/cm in the strong axis is utilized. When each MOT is operated separately, a He* MOT of 3×10^8 atoms at 1 mK and a ^{87}Rb MOT of 3×10^8 atoms at 100 μK is routinely obtained. When the ^{87}Rb MOT is operated with the He* source on, the number drops to ~5×10^7 atoms.

We use a saturated fluorescence method [16] to determine the He* atom number. The method relies on ramping the MOT laser beams to resonance with full power. In the case of He*, we use an intensity hundreds of times greater than saturation, and thus, atoms scatter at close to the maximum rate of $\Gamma/2$. This method is insensitive to the atomic distribution among magnetic sublevels, so one need only take into account the collection efficiency of the imaging system to determine the number of atoms. A typical saturated fluorescence peak is shown in the inset of Fig. 3. The saturated fluorescence method results in the destruction of the MOT. Therefore, this method cannot be used while monitoring the number decay of the ^{87}Rb MOT. Instead the number is simply calculated from the fluorescence emitted as the MOT decays. The disadvantage of this method is that the error is much greater as the unsaturated fluorescence level is sensitive to the magnetic sublevel population distribution and laser intensity.

The trap loading and decay curves are measured by monitoring the atom fluorescence. Separate photodiodes with appropriate bandpass filters are used to monitor the He* and
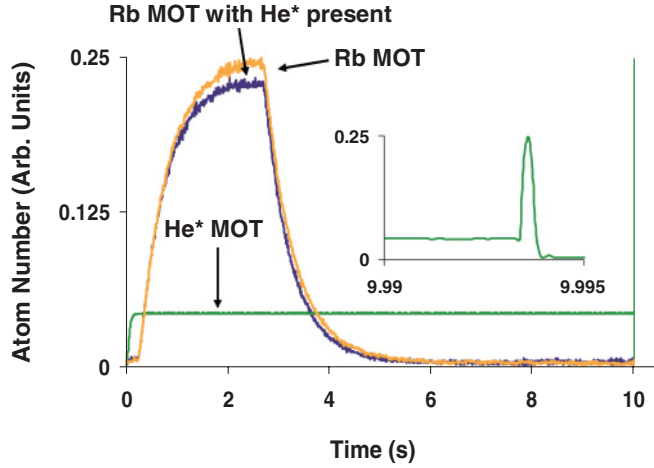
FIG. 3. (Color online) Typical photodiode traces with the loading and decay of a ^{87}Rb MOT, a He* MOT, and ^{87}Rb MOT with a He* MOT present. Loss in the ^{87}Rb MOT due to the He* MOT can clearly be seen. The inset shows a saturated fluorescence measurement of the He* number.

^{87}Rb fluorescence, respectively. CCD cameras are also placed on the top and side of the chamber. Using images from these cameras, the overlap of the clouds can be maximized in every direction and the widths of the clouds can be measured.

III. TRAP LOSS

The decay of the number of trapped ^{87}Rb atoms in a dual-species ^{87}Rb-He* MOT is given by

$$\frac{dN_{\text{Rb}}}{dt} = -\alpha N_{\text{Rb}} - \beta \int_V n_{\text{Rb}}^2 d^3r - \beta_{\text{Rb-He}^*} \int_V n_{\text{Rb}} n_{\text{He}^*} d^3r,$$

(2)

where α is the loss rate due to collisions between trapped ^{87}Rb atoms and hot background atoms, β is the loss rate due to cold collisions between trapped ^{87}Rb atoms, $\beta_{\text{Rb-He}^*}$ is the loss rate due to collisions between trapped ^{87}Rb atoms and trapped He* atoms, and n is the atomic density.

The spatial distribution for both ^{87}Rb and He* in the MOT is well described by a Gaussian distribution, and as neither MOT reaches the density-limited regime, $n(r, t)$ can be written as [17]

$$n(r, t) = n_0(t)e^{-r^2/2\sigma^2},$$

(3)

where σ is the rms radii of the cloud. Substituting Eq. (3) into Eq. (2) and integrating over the volume results in

$$\frac{dN_{\text{Rb}}}{dt} = -\alpha' N_{\text{Rb}} - \frac{\beta}{\left(4\sigma_{\text{Rb}}^2 \pi\right)^{3/2}} N_{\text{Rb}}^2,$$

(4)

where

$$\alpha' = \alpha + \beta_{\text{Rb-He}^*} N_{\text{He}^*} \left[\frac{1}{2\pi \left(\sigma_{\text{Rb}}^2 + \sigma_{\text{He}^*}^2\right)}\right]^{3/2}.$$

(5)

Integrating Eq. (4) with respect to time yields

$$N_{\text{Rb}}(t) = \frac{\left(4\pi \sigma_{\text{Rb}}^2\right)^{3/2} \alpha' N_{\text{Rb}}(0)}{\left[\left(4\pi \sigma_{\text{Rb}}^2\right)^{3/2} \alpha' + \beta N_{\text{Rb}}(0)\right] e^{(\alpha' t)} - \beta N_{\text{Rb}}(0)}.$$

(6)

The experimental procedure to measure $\beta_{\text{Rb-He}^*}$ is as follows. First, separate He* and Rb MOTs are allowed to load to steady-state values; σ_{Rb} and σ_{He^*} are then found using the CCD cameras. Next a ^{87}Rb MOT is loaded to a steady-state value, the loading is stopped (by blocking the LVIS light), and the ^{87}Rb MOT is allowed to decay naturally while the fluorescence is recorded. By fitting Eq. (6) (with $\beta_{\text{Rb-He}^*} = 0$) to this data, β and α can be found. It should be noted that the ^{87}Rb MOT is allowed to load and decay in the presence of the background from the source. This is necessary to ensure consistency in the conditions between the single MOT and the dual MOT (the only change is the presence of a He* MOT).

Finally the He* and ^{87}Rb MOTs are both loaded to a steady-state value. While the He* MOT is kept at this steady state, the ^{87}Rb MOT is allowed to decay and again the fluorescence is recorded. Once the ^{87}Rb MOT has fully decayed, a He* saturated fluorescence measurement is taken to determine N_{He^*}. Equation (6) is then fitted to the decay curve and $\beta_{\text{Rb-He}^*}$ can be found.

Figure 3 shows typical photodiode traces of the loading and decay of the ^{87}Rb MOT with and without a He* MOT present. It also shows the typical loading of a He* MOT and a saturated fluorescence measurement of the He* number which results in the destruction of the He* MOT.

IV. RESULTS

Approximately 5×10^7 ^{87}Rb atoms are loaded into the MOT and allowed to decay. A least-squares fit of Eq. (6) to the ^{87}Rb decay curve yields $\alpha = 1.69$ s^{-1}. As the ^{87}Rb two-body decay, β_{Rb}, is below the noise level, a value of $\beta_{\text{Rb}} = 2 \times 10^{-12}$ cm^3/s was taken from the literature [11]. The high value of α is due to the large background produced from the source that copropagates with the He* beam.

With the single- and dual-species behavior characterized, we monitor the decay of a ^{87}Rb MOT in the presence of a He* MOT consisting of 4×10^7 atoms. Figure 4 shows averaged photodiode traces of the decay of the ^{87}Rb MOT with and without a He* MOT present along with the fits to
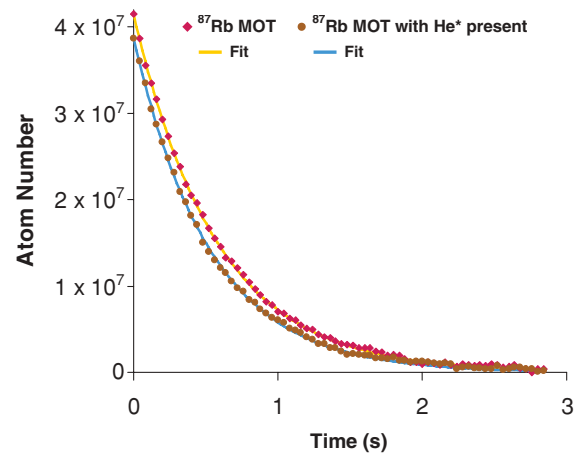

FIG. 4. (Color online) Averaged ^{87}Rb MOT decay with and without a He* MOT present; fitting to these curves yields α, β, and $\beta_{\text{Rb-He}^*}$. Some points have been removed to improve clarity.

these curves. Using Eq. (6), $\beta_{\text{Rb-He}^*}$ is found to be $\beta_{\text{Rb-He}^*} = (6 \pm 2) \times 10^{-10}$ cm^3/s. The greatest source of error in the measurement is from uncertainty in the ^{87}Rb number.

This result is smaller than the light-assisted, S-P, β_{He^*} of $(1.9 \pm 0.8) \times 10^{-9}$ cm^3/s [10], and is similar to the S-S $\beta_{\text{He}^*} = (1.3 \pm 2) \times 10^{-10}$ cm^3/s [18]. This is not an unexpected result. For colliding homonuclear atoms in the S state, the interatomic potential is predominantly characterized by the $1/R^6$ van der Waals interaction. If during the collision one of the atoms is excited and the collision is now between an S and a P state atom, the interaction is governed by the much longer range $1/R^3$ dipole-dipole interaction. Thus, an S-P collision between two homonuclear atoms will typically result in a higher loss rate than an S-S collision. However, for a heteronuclear excited-ground-state collision, the interaction occurs predominantly on a $1/R^6$ potential. Thus, a light-assisted ^{87}Rb-He* collision is predominantly governed by the same interaction potential as a ground-state He*-He* collision. It should also be noted that $\beta_{\text{Rb-He}^*}$ is found to lie approximately halfway between β_{He^*} and β_{Rb}. This is similar to the ^{85}Rb-Ar* result of $\beta_{^{85}\text{Rb}-\text{Ar}^*} = 3.1 \times 10^{-11}$ cm^3/s which lies approximately midway between $\beta_{\text{Ar}^*} = 5.8 \times 10^{-10}$ cm^3/s and $\beta_{\text{Rb}^{85}} = 3.7 \times 10^{-12}$ cm^3/s [7]. To the best of our knowledge, there is currently no theoretical potential interaction curves for ^{87}Rb-He*. We hope that this experimental result will stimulate theoretical interest in calculating the interaction potentials.

V. CONCLUSION

In conclusion, we have demonstrated simultaneous magneto-optical trapping of ^{87}Rb and He* and have measured the two-body, light-assisted loss rate to be $\beta_{\text{Rb-He}^*} = (6 \pm 2) \times 10^{-10}$ cm^3/s.

This high loss rate seems to preclude the possibility of creating a dual-species ^{87}Rb-He* condensate; however, the same mechanism that makes it possible to create a He* condensate, spin suppression of Penning ionization, should be present in a ^{87}Rb-He* mixture. If the whole mixture is spin-polarized (He* in the $m_j = +1$ and ^{87}Rb in the $m_f = +2$), Penning ionization should be reduced as spin conservation cannot be satisfied (the total spin of the colliding particles in the initial state equals 3, while the total spin in the final case does not exceed 2). However, it is unclear what the extent of the suppression will be as the interaction potentials of the mixture are not known. In spin-polarized He*, a factor of $\sim 10^4$ suppression is observed [19]. A similar value would be needed to create a ^{87}Rb-He* BEC.

In the near future we intend to measure the spin suppression of Penning ionization in a polarized ^{87}Rb-He* mixture. To do this, we mean to monitor the ions produced from Penning collisions. By measuring the ion production rate in the unpolarized case (ions from the MOT) versus the ion production rate in the polarized case (ions from the magnetic trap), the spin suppression factor can be determined. We also plan to investigate the elastic scattering rates between the ^{87}Rb and the He*. If these rates prove favorable, we can use the ^{87}Rb as a thermal bath for the He*, allowing us to create a large number of He* condensates.

[1] U. Schloder, H. Engler, U. Schunemann, R. Grimm, and M. Weidemuller, Eur. Phys. J. D **7**, 331 (1999).

[2] M.-O. Mewes, G. Ferrari, F. Schreck, A. Sinatra, and C. Salomon, Phys. Rev. A **61**, 011403(R) (1999).

[3] T. Takekoshi, B. M. Patterson, and R. J. Knize, Phys. Rev. A **59**, R5 (1999).

[4] S. B. Papp, J. M. Pino, and C. E. Wieman, Phys. Rev. Lett. **101**, 040402 (2008).

[5] M. Mancini, A. Caires, G. Telles, V. Bagnato, and L. Marcassa, Eur. Phys. J. D **30**, 105 (2004).

[6] S. Hensler, A. Griesmaier, J. Werner, A. Görlitz, and T. Pfau, J. Mod. Opt. **51**, 1807 (2004).

[7] H. C. Busch, M. K. Shaffer, E. M. Ahmed, and C. I. Sukenik, Phys. Rev. A **73**, 023406 (2006).

[8] Y. Torii, N. Shiokawa, T. Hirano, T. Kuga, Y. Shimizu, and H. Sasada, Eur. Phys. J. D **1**, 239 (1998).

[9] F. Pereira Dos Santos, J. Léonard, J. Wang, C. J. Barrelet, F. Perales, E. Rasel, C. S. Unnikrishnan, M. Leduc, and C. Cohen-Tannoudji, Phys. Rev. Lett. **86**, 3459 (2001).

[10] H. C. Mastwijk, J. W. Thomsen, P. van der Straten, and A. Niehaus, Phys. Rev. Lett. **80**, 5516 (1998).

[11] S. D. Gensemer, V. Sanchez-Villicana, K. Y. N. Tan, T. T. Grove, and P. L. Gould, Phys. Rev. A **56**, 4055 (1997).

[12] J. A. Swansson, K. G. H. Baldwin, M. D. Hoogerland, A. G. Truscott, and S. J. Buckman, Appl. Phys. B **79**, 485 (2004).

[13] L. J. Uhlmann, R. G. Dall, A. G. Truscott, M. D. Hoogerland, K. G. H. Baldwin, and S. J. Buckman, Phys. Rev. Lett. **94**, 173201 (2005).

[14] R. J. W. Stas, J. M. McNamara, W. Hogervorst, and W. Vassen, Phys. Rev. A **73**, 032713 (2006).

[15] K. Dieckmann, R. J. C. Spreeuw, M. Weidemüller, and J. T. M. Walraven, Phys. Rev. A **58**, 3891 (1998).

[16] M. T. DePue, S. L. Winoto, D. J. Han, and D. S. Weiss, Opt. Commun. **180**, 73 (2000).

[17] F. P. D. Santos, F. Perales, J. Léonard, A. Sinatra, J. Wang, F. S. Pavone, E. Rasel, C. Unnikrishnan, and M. Leduc, Eur. Phys. J. D **14**, 15 (2001).

[18] P. J. J. Tol, N. Herschbach, E. A. Hessels, W. Hogervorst, and W. Vassen, Phys. Rev. A **60**, R761 (1999).

[19] O. Sirjean, S. Seidelin, J. V. Gomes, D. Boiron, C. I. Westbrook, A. Aspect, and G. V. Shlyapnikov, Phys. Rev. Lett. **89**, 220406 (2002).